

---

# RegD: Hierarchical Embeddings via Distances over Geometric Regions

---

Hui Yang<sup>1</sup> Jiaoyan Chen<sup>1</sup>

## Abstract

Hierarchical data are common in many domains like life sciences and e-commerce, and their embeddings often play a critical role. Although hyperbolic embeddings offer a grounded approach to representing hierarchical structures in low-dimensional spaces, their utility is hindered by optimization difficulties in hyperbolic space and dependence on handcrafted structural constraints. We propose RegD, a novel Euclidean framework that addresses these limitations by representing hierarchical data as geometric regions with two new metrics: (1) depth distance, which preserves the representational power of hyperbolic spaces for hierarchical data, and (2) boundary distance, which explicitly encodes set-inclusion relationships between regions in a general way. Our empirical evaluation on diverse real-world datasets shows consistent performance gains over state-of-the-art methods and demonstrates RegD’s potential for broader applications beyond hierarchy alone tasks.

## 1. Introduction

Embedding discrete data into low-dimensional vector spaces has become a cornerstone of modern machine learning. In Natural Language Processing (NLP), seminal works such as word2vec (Mikolov et al., 2013) and GloVe (Pennington et al., 2014) represent words as vectors to capture intricate linguistic relationships. Similarly, knowledge graph embedding methods (Bordes et al., 2013; Sun et al., 2019; Balazevic et al., 2019) encode entities and relations as vectors with their semantics concerned to facilitate reasoning and prediction.

Our work focuses on embedding hierarchical data into low-dimensional spaces. Such data represents partial orders over sets of elements, denoted as  $u \prec v$ , where  $u$  is a par-

ent of  $v$ . These partial orders naturally manifest as trees or directed acyclic graphs (DAGs). The ability to effectively embed such hierarchical structures enables crucial operations like inferring sub- or superclasses of concepts and classifying nodes within graphs. These capabilities are essential for various tasks in knowledge management and discovery, particularly towards knowledge bases (Shi et al., 2024; Abboud et al., 2020), ontologies (He et al., 2024a; Chen et al., 2024) and taxonomies (Shen & Han, 2022).

Current methods for embedding hierarchical data can be broadly categorized into two paradigms: *region-based* and *hyperbolic* approaches. The region-based approach usually represents entities as geometric regions in the Euclidean space, capturing hierarchical relationships through intuitive region-inclusion. However, these methods often experience degraded performance in low-dimensional settings due to the crowding effect inherent in Euclidean spaces.

In contrast, the hyperbolic approach takes advantage of the unique geometric properties of hyperbolic spaces – specifically their exponential growth in distance and volume – enabling more effective embeddings of tree-structured data in low dimensions. However, existing hyperbolic methods often rely on specialized constructions informed by theoretical analysis or physical models (Ganea et al., 2018; Yu et al., 2024), limiting their applicability beyond strictly hierarchical data. Additionally, training in hyperbolic space is challenging due to precision issues and the complexities of Riemannian optimization.

In this paper, we propose a flexible framework named RegD for modeling hierarchical data by embedding arbitrary regions in Euclidean spaces. Our framework relies on two novel distance metrics, *depth distance* and *boundary distance*, which combine the strengths of both region-based approaches in Euclidean spaces and hyperbolic methods.

- The depth distance (cf. Section 3) enables our model to achieve similar embedding expressivity to hyperbolic spaces by incorporating the “size” of the regions under consideration. Its computation involves only simple operations, thereby reducing computational complexity and eliminating the need for enhanced numerical precision required by hyperbolic methods.
- The boundary distance (cf. Section 4) improves the rep-

---

<sup>1</sup>Department of Computer Science, The University of Manchester, Manchester, UK. Correspondence to: Hui Yang <hui.yang-2@manchester.ac.uk>, Jiaoyan Chen <jiaoyan.chen@manchester.ac.uk>.

representation of set-inclusion relationships among regions in Euclidean spaces. This allows for better identification of shallower and deeper descendants, thereby capturing hierarchical structures more effectively than traditional region-based approaches.

Combining these two distances, we designed a closed formula (cf. Section 5) for determining the partial order of two concepts based on their embedded regions, which is used in both the training and evaluation processes.

Notably, RegD can be applied to arbitrary regions, including common geometric representations such as balls (hyperspheres) and boxes (hyperrectangles). This generality enables broad applicability across diverse geometric embeddings for various tasks, extending beyond hierarchy alone data to ontologies that include hierarchies and more complex relationships in Description Logic (Baader et al., 2017) (cf. Sections 6.2 and 6.3). Our main contributions are summarized as follows:

- We present a versatile framework that is able to embed hierarchical data as arbitrary regions in Euclidean space.
- We offer a rigorous theoretical analysis demonstrating that our framework retains the core embedding benefits of hyperbolic methods.
- Experiments on diverse real-world datasets demonstrate that our framework consistently outperforms existing approaches on embedding hierarchies and ontologies for reasoning and prediction.

## 2. Preliminaries and Related Works

**Manifold and Hyperbolic Space** A  $d$ -dimensional *manifold* (Lee, 2013), denoted  $\mathcal{M}$ , is a hypersurface embedded in an  $n$ -dimensional Euclidean space,  $\mathbb{R}^n$ , where  $n \geq d$ , and locally resembles  $\mathbb{R}^d$ . A *Riemannian manifold*  $\mathcal{M}$  is a manifold equipped with a Riemannian metric, enabling the definition of a distance function  $d_{\mathcal{M}}(\mathbf{x}, \mathbf{y})$  for  $\mathbf{x}, \mathbf{y} \in \mathcal{M}$ . *Hyperbolic space*, denoted  $\mathbb{H}^n$ , is a Riemannian manifold with a constant negative curvature of  $-k$ , where  $k > 0$  (Lee, 2006). It can be represented using various isometric models, such as the Poincaré half-space model, where the points are defined by the half-space:  $U^n = \{\mathbf{x} \in \mathbb{R}^n : x_n > 0\}$ , and the hyperbolic distance between  $\mathbf{x}, \mathbf{y} \in U^n$  is given by

$$d_{\mathbb{H}}(\mathbf{x}, \mathbf{y}) = \frac{1}{\sqrt{k}} \operatorname{arcosh} \left( 1 + \frac{\|\mathbf{x} - \mathbf{y}\|_2^2}{2x_n y_n} \right).$$

**Region-based Methods** Region-based methods embed the nodes of a directed acyclic graph (DAG) into geometric regions, such as boxes (Boratko et al., 2021), balls

(Suzuki et al., 2019), and cones (Vendrov et al., 2016), capturing hierarchical relationships through set-inclusion between these regions. Training is typically conducted using an inclusion loss, which is often defined in terms of the distance or volume of the regions (Vendrov et al., 2016). However, such loss functions may involve non-smooth operations, like maximization, which have been addressed through probabilistic (Vilnis et al., 2018; Dasgupta et al., 2020) or smooth (Boratko et al., 2021) approximations to improve performance.

Due to the crowding effect in the Euclidean space, region-based methods could exhibit suboptimal performance in low-dimensional spaces or when representing large DAGs. To address this challenge, Suzuki et al. (2019) proposed using balls on Riemannian manifolds, enabling more flexible shapes beyond the canonical balls used in Euclidean space. However, leveraging Riemannian manifolds introduces more complex optimization and training processes, which can struggle with tasks beyond hierarchical structures. This makes the approach more restrictive compared to ours, which offers broader applicability.

While Boratko et al. (2021) demonstrates that box-based embeddings in Euclidean spaces can represent any DAG, their focus is on reconstructing DAGs rather than preserving the graph’s transitive properties. Consequently, this approach does not guarantee the faithful capture of hierarchical semantics unless all transitive closure edges are included in the training data.

**Hyperbolic Methods** Hyperbolic space embeddings were first introduced for modeling hierarchical structures by (Nickel & Kiela, 2017). This approach combines hyperbolic distance with the Euclidean norm to represent hierarchies. However, it does not explicitly capture hierarchical relationships and struggles to model the transitivity inherent in these structures. To address these limitations, EntailmentCones (Ganea et al., 2018) and ShadowCones (Yu et al., 2024) were proposed. These methods enhance hierarchy modeling by constructing specific cones in a hyperbolic space: EntailmentCones introduced closed-form hyperbolic cones, determined by their apex coordinates, to ensure transitivity, while ShadowCones is inspired by the physical interplay of light and shadow.

Despite the representational power of hyperbolic spaces, training in non-Euclidean spaces poses unique challenges. Precision-related issues, for example, often arise near the boundaries of the Poincaré half-space model, necessitating high-precision tensor operations that increase both storage requirements and computation time. Moreover, achieving optimal performance in hyperbolic spaces typically requires specialized training techniques, such as burn-in strategies (Yu et al., 2024), custom initialization meth-

ods (Ganea et al., 2018), or gradient descent algorithms adapted to Riemannian manifolds (Bécigneul & Ganea, 2019).

### 3. Depth Distance: Similarly Distance Considering Depth

Unlike the Euclidean space, which is constrained by crowding effects that limit its embedding capacity, the hyperbolic space leverage exponential growth in distance and volume to offer superior embedding capabilities. This property makes the hyperbolic space particularly effective for representing tree-structured data in low-dimensional spaces. Notably, two key distinctions arise between region-based embeddings in the Euclidean space and hyperbolic embeddings:

1. *The hyperbolic space better discriminate different hierarchical layers than the Euclidean space.*

Consider the taxonomy illustrated in Figure 1 (left). Intuitively, since *human* is a subcategory of *animal*, the semantic difference between *human* and *plant* should be greater than that between *animal* and *plant*. The hyperbolic space effectively captures this hierarchical relationship by permitting  $d(v_{human}, v_{plant}) > d(v_{animal}, v_{plant}) + \Delta$ , where  $\Delta$  is an arbitrary gap. This arises from the property that the distance metric diverges to infinity near the boundary, as illustrated by the shadow dense of the bar on the left-hand side of  $\mathbb{H}^2$  in Figure 1 (middle). In contrast, region-based embeddings on Euclidean space may violate this hierarchical constraint, potentially placing the box  $B_{human}$  close to  $B_{plant}$ , resulting in a distance (e.g., the Euclidean distance between box centers) similar to or even smaller than that between  $B_{animal}$  and  $B_{plant}$ .

2. *The hyperbolic space enable the distinct representation of an arbitrary number of child nodes.*

As demonstrated in Figure 1, the box embeddings in the Euclidean space face inherent limitations when representing multiple children of a node such as *animal*. As the number of children increases, their corresponding boxes must cluster within  $B_{animal}$ , leading to crowding. In contrast, the hyperbolic space can accommodate an arbitrary number of children while maintaining distinct separations between them. This capability arises from the exponential growth of distance near the boundary of the hyperbolic space, which allows unlimited child nodes to be positioned distinctly by placing them progressively closer to the boundary while preserving meaningful distances between them.

In the following sections, we introduce the *depth distance* for regions in Euclidean space which considers the “size”

of regions. We demonstrate that this measure exhibits advantages similar to those of hyperbolic spaces discussed above (Theorem 1), while maintaining a simpler structure that facilitates implementation. Furthermore, we prove that our depth distance can be equivalent to hyperbolic distance when using specific nonlinear functions, and even with simple polynomial functions, it preserves key properties of hyperbolic geometry (Propositions 1, 2).

#### 3.1. Construction

The depth distance serves as a similarity measure that quantifies the relationship between objects considering their hierarchical depth. As we use set-inclusion relations to model the hierarchy, this hierarchical depth can be represented through the size of the regions, such as their volumes or diameters. Formally, the depth distance is defined as follows, where the size of the regions is represented by a function  $f(\text{reg})$ :

**Definition 1** (Depth Distance). *Let  $\mathcal{R}$  be a collection of regions in the  $n$ -dimensional Euclidean space  $\mathbb{R}^n$ , where each region  $\text{reg} \in \mathcal{R}$  is characterized by an  $m$ -dimensional parameter  $\text{par}(\text{reg}) \in \mathbb{R}^m$ . The depth-aware similarity distance between two regions  $\text{reg}_1, \text{reg}_2 \in \mathcal{R}$ , is defined as:*

$$d_{\text{dep}}(\text{reg}_1, \text{reg}_2) = g \left( \frac{\|\text{par}(\text{reg}_1) - \text{par}(\text{reg}_2)\|_p^p}{f(\text{reg}_1)f(\text{reg}_2)} \right) \quad (1)$$

where  $\|\cdot\|_p$  is the  $p$ -norm (i.e.,  $\|\mathbf{x}\|_p = (\sum_i \mathbf{x}_i^p)^{1/p}$ ), and:

- $g : \mathbb{R}_{\geq 0} \rightarrow \mathbb{R}_{\geq 0}$  is an increasing function such that  $g(x) = 0$  if and only if  $x = 0$ ,
- $f : \mathcal{R} \rightarrow \mathbb{R}_{> 0}$  is a function that measures the size of regions. It satisfies:  $\lim_{\text{reg} \rightarrow \emptyset} f(\text{reg}) = 0^1$ .

We require  $f$  and  $g$  to have non-negative values to ensure the depth distance is non-negative. Additionally, we stipulate that  $\lim_{\text{reg} \rightarrow \emptyset} f(\text{reg}) = 0$  to guarantee that as a region shrinks to an empty set, the distance between this object and others can approach infinity. This setting emulates the beneficial properties of the hyperbolic space, where the distance between two points can grow rapidly as they approach the boundary of the space (i.e.,  $\mathbf{x}_n = 0$  in the Poincaré half-space model). In our context, the boundary of the space  $\mathcal{R}$  of a collection of (parametrized) regions in the Euclidean space is the empty set. By selecting an appropriate function  $f$ , we can control the rate at which the distance between two objects increases as they approach this boundary.

<sup>1</sup>Here,  $\text{reg} \rightarrow \emptyset$  indicates that the region  $\text{reg}$  approaches an empty set, which can be characterized by its volume or other relevant measures.

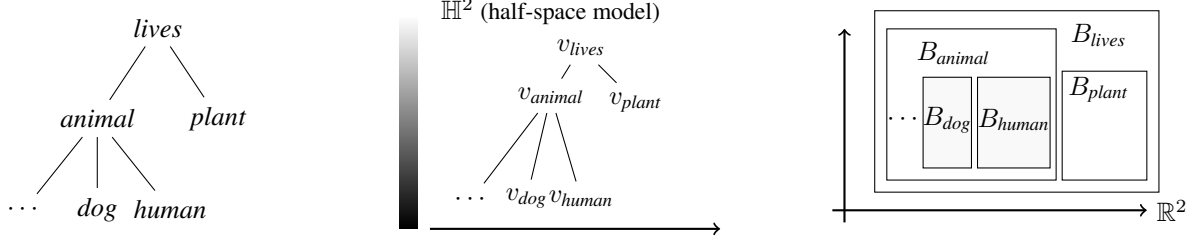


Figure 1. Demonstration of a taxonomy (left), its embeddings in the hyperbolic space (middle) and in the Euclidean space as boxes (right).

**Example 1.** Consider ball defined by a center  $\mathbf{c} \in \mathbb{R}^n$  and a radius  $r > 0$  as:

$$\text{ball}(\mathbf{c}, r) = \{\mathbf{x} \mid \|\mathbf{x} - \mathbf{c}\| \leq r\}.$$

Given two such balls,  $\text{ball}_1$  and  $\text{ball}_2$ , by setting  $g(x) = x$  and  $f(\text{ball}) = h(\text{ball}) \cdot r$ , where  $h$  is an arbitrary function defined by the parameters of balls, we obtain their depth distance as:

$$d_{\text{dep}}(\text{ball}_1, \text{ball}_2) = \frac{\|\mathbf{c}_1 - \mathbf{c}_2\|_p^p + |r_1 - r_2|^p}{(h(\text{ball}_1) \cdot r_1) \cdot (h(\text{ball}_2) \cdot r_2)}. \quad (2)$$

**Example 2.** Consider box defined by a center  $\mathbf{c} \in \mathbb{R}^n$  and an offset  $\mathbf{o} \in \mathbb{R}_{>0}^n$  as follows:

$$\text{box}(\mathbf{c}, \mathbf{o}) = \{\mathbf{x} \in \mathbb{R}^n \mid \mathbf{c} - \mathbf{o} \leq \mathbf{x} \leq \mathbf{c} + \mathbf{o}\}.$$

Given two such boxes,  $\text{box}_1$  and  $\text{box}_2$ , by setting  $g(x) = x$  and  $f(\text{box}) = h(\text{box}) \cdot \|\mathbf{o}\|$ , we obtain the depth distance as:

$$d_{\text{dep}}(\text{box}_1, \text{box}_2) = \frac{\|\mathbf{c}_1 - \mathbf{c}_2\|_p^p + \|\mathbf{o}_1 - \mathbf{o}_2\|_p^p}{(h(\text{box}_1) \cdot \|\mathbf{o}_1\|) \cdot (h(\text{box}_2) \cdot \|\mathbf{o}_2\|)}. \quad (3)$$

The following result highlights that the depth distance exhibits properties analogous to those of the hyperbolic distance discussed earlier in this section. Specifically, the depth distance (1) effectively distinguishes concepts across different layers of the hierarchy with an arbitrary separation gap, denoted by  $\Delta$  in item 1 of the following Theorem 1, and (2) distinctly represents an arbitrary number  $n$  of children within a single parent by a distance greater than  $M$ , as demonstrated in item 2 of the theorem.

**Theorem 1.** Consider the region space  $\mathcal{B}^n$  consisting of balls in  $\mathbb{R}^n$ , with the depth distance defined in Example 1. The following properties hold:

1. For any  $\text{ball}_1, \text{ball}_2 \in \mathcal{B}^n$  and any  $\Delta > 0$ , there exists a positive constant  $r_0$  such that for any  $\text{ball}(\mathbf{c}', r') \subseteq \text{ball}_2$ , if  $r' \leq r_0$ , then

$$d_{\text{dep}}(\text{ball}_1, \text{ball}(\mathbf{c}', r')) > d_{\text{dep}}(\text{ball}_1, \text{ball}_2) + \Delta.$$

2. For any ball  $\in \mathcal{B}^n$ , any integer  $n$  and any  $M > 0$ , there exist subsets  $\text{ball}_1, \dots, \text{ball}_n \subseteq \text{ball}$  such that

$$d_{\text{dep}}(\text{ball}_i, \text{ball}_j) > M$$

for any distinct  $i, j \in \{1, \dots, n\}$ .

The same conclusions hold for boxes, where  $r_0 \in \mathbb{R}_{>0}$  is replaced with  $\mathbf{o}_0 \in (\mathbb{R}_{>0})^n$ , and the condition  $r' \leq r_0$  is replaced by  $\mathbf{o}' \leq \mathbf{o}_0$  element-wise.

Notably, the results established in Theorem 1 naturally generalize to other parameterized regions, with proofs following analogous arguments. Here, we restrict our analysis to boxes and balls due to their well-defined geometric parameters, which allow for clear mathematical formulation and analysis.

### 3.2. Comparison with the Hyperbolic Distance

By choosing appropriate functions  $f$  and  $g$ , we can construct a region space that is equivalent to the hyperbolic space, as demonstrated by the following theorem.

**Proposition 1.** Let  $\mathbb{H}^{n+1}$  be the hyperbolic space with curvature  $-1$ . Assume the ball space  $\mathcal{B}^n$  is parameterized as in Example 1, and equipped with the depth distance defined in Equation (1). Then the map

$$F: \quad \mathcal{B}^n \rightarrow \mathbb{H}^{n+1}$$

$$\text{ball}(\mathbf{c}, r) \mapsto [\mathbf{c} : r]$$

is an bijective isometry when  $p = 2$ ,  $g(x) = \text{arcosh}(x+1)$ , and  $f(\text{ball}(\mathbf{c}, r)) = \sqrt{2}r$ .

**Remark 1.** The mapping  $F$  above can be generalized to arbitrary regions. For example, we could extend  $F$  by replacing the center point and radius of balls with the center of gravity and diameters of any region. However, in this case, the function  $F$  might be non-injective, as distinct regions may share the same center of gravity and diameters. Therefore, the resulting region space serves more as an extension rather than an equivalence of hyperbolic space.

Moreover, the following result demonstrates that even with simple linear function  $g(\cdot)$ , our depth distance retains the



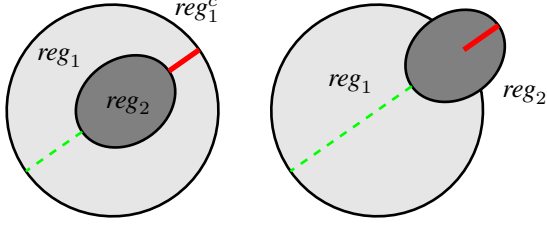


Figure 2. Illustration of the boundary distances between  $reg_1$  and  $reg_2$  in two cases:  $reg_2 \subseteq reg_1$  (left) and  $reg_2 \not\subseteq reg_1$  (right).

ability to capture the hyperbolic structure. Specifically, there exists a map from the region space to the hyperbolic space that preserves the order of hyperbolic distances for all pairs of points, as stated below.

**Proposition 2.** *Following Proposition 1, let the depth distance  $d_{dep}$  be redefined by replacing  $g$  to  $g(x) = k \cdot x + b$  ( $k > 0$ ). Then the map  $F$  retains the following monotonicity property: for any points  $\mathbf{x}_1, \mathbf{x}_2, \mathbf{x}_3, \mathbf{x}_4 \in \mathbb{H}^n$ ,*

$$d_{\mathbb{H}^n}(\mathbf{x}_1, \mathbf{x}_2) < d_{\mathbb{H}^n}(\mathbf{x}_3, \mathbf{x}_4)$$

if and only if

$$d_{dep}(F^{-1}(\mathbf{x}_1), F^{-1}(\mathbf{x}_2)) < d_{dep}(F^{-1}(\mathbf{x}_3), F^{-1}(\mathbf{x}_4)).$$

Therefore, by using only elementary arithmetic operations, our depth distance shares similar embedding capabilities to those of hyperbolic spaces. This offers two key advantages over hyperbolic approaches: (1) our method eliminates the need for high-precision numerical representations, such as double-precision tensors (`DoubleTensor`), which can increase computational complexity and memory usage; and (2) our approach does not require specialized training strategies tailored to the hyperbolic space, which are often essential for achieving optimal performance in hyperbolic space models.

## 4. Boundary Distance: Non-Symmetric Distance for Inclusion

Although the depth distance  $d_{dep}$  introduced above has been shown to have great power for embedding hierarchical data, it is a symmetric distance and therefore inadequate for fully capturing the inherently non-symmetric hierarchical relationships between objects. To address this limitation, we introduce the boundary distance, specifically designed to reflect the partial order of regions defined by set inclusion.

To the best of our knowledge, the concept of boundary distance was first introduced and applied to the embedding of hierarchical data by ShadowCone (Yu et al., 2024). However, their construction is limited to specific types of cones defined in hyperbolic space, and its computation requires

specialized functions (e.g.,  $\text{arcsinh}$ ), which introduce additional computational costs. In contrast, we propose a more general construction of the boundary distance that can be applied to arbitrary regions in the Euclidean space. Furthermore, our approach is computationally efficient for commonly used geometric objects, such as balls and boxes, requiring only basic arithmetic operations.

### 4.1. Construction

The boundary distance is defined to measure the minimal cost associated with transforming the spatial relationship between two regions  $reg_1$  and  $reg_2$ . Specifically, it quantifies the cost of moving  $reg_2$  out of  $reg_1$  when  $reg_2 \subseteq reg_1$ , or moving  $reg_2$  into  $reg_1$  otherwise (when  $reg_2 \not\subseteq reg_1$ ). This cost can be defined for arbitrary geometric objects based on either distance or volume within Euclidean or other spaces. Below, we introduce a boundary distance based on the Euclidean distance for two regions  $reg_1, reg_2 \subseteq \mathbb{R}^n$ , which consists of two cases:

1. *Containment ( $reg_2 \subseteq reg_1$ ):* As illustrated in the left of Figure 2, when  $reg_2$  is fully contained within  $reg_1$ , the boundary distance is defined by the minimum Euclidean distance between the complementary region  $reg_1^c$  and the points in  $reg_2$  (i.e., length of the red line). This distance quantifies the minimum translation cost required to move at least a part of  $reg_2$  out of  $reg_1$ .
2. *Non-Containment ( $reg_2 \not\subseteq reg_1$ ):* As shown in the right of Figure 2, when  $reg_2$  is not fully contained within  $reg_1$ , the boundary distance is defined as the maximum Euclidean distance from the points in  $reg_2 \setminus reg_1$  to  $reg_1$  (i.e., length of the red line). This distance quantifies the minimum translation cost for moving  $reg_2$  into  $reg_1$ .

Let  $d(\mathbf{x}, reg) := \min\{\|\mathbf{x} - \mathbf{y}\| \mid \mathbf{y} \in reg\}$  be the distance of a points  $\mathbf{x}$  to a region  $reg$  defined by the minimal distance from  $\mathbf{x}$  to  $\mathbf{y} \in reg$ . The formal definition of the boundary distance is as follows:

**Definition 2** (Boundary Distance). *Given a region space  $\mathcal{R}$ , we define the boundary distance over  $reg_1, reg_2 \in \mathcal{R}$  by:*

$$d_{bd}(reg_1, reg_2) = \begin{cases} -\min_{\mathbf{x}_2 \in reg_2} \{d(reg_1^c, \mathbf{x}_2)\} & \text{if } reg_2 \subseteq reg_1 \\ \max_{\mathbf{x}_2 \in reg_2 \setminus reg_1} \{d(reg_1, \mathbf{x}_2)\} & \text{else.} \end{cases} \quad (4)$$

Note that a negative sign is added to  $d_{bd}(reg_1, reg_2)$  in the containment case ( $reg_2 \subseteq reg_1$ ) to clearly distinguish it from other cases. Moreover, the boundary distance is inherently asymmetric, that is,  $d_{bd}(reg_1, reg_2) \neq d_{bd}(reg_2, reg_1)$  in general. For example, as illustrated in Figure 2, the

boundary distance in the reverse order,  $d_{bd}(reg_2, reg_1)$ , corresponds to the length of the green dashed line, which differs from the red line representing  $d_{bd}(reg_1, reg_2)$ .

Moreover, for widely used geometric objects such as balls and boxes, the boundary distance can be computed efficiently using simple arithmetic operations.

**Example 3.** If  $reg_1 = ball(\mathbf{c}_1, r_1)$  and  $reg_2 = ball(\mathbf{c}_2, r_2)$ , the boundary distance have the form:

$$d_{bd}(reg_1, reg_2) = \|\mathbf{c}_1 - \mathbf{c}_2\|_2 + r_2 - r_1$$

For the case of boxes, where  $reg_1 = box(\mathbf{c}_1, \mathbf{o}_1)$  and  $reg_2 = box(\mathbf{c}_2, \mathbf{o}_2)$ , the boundary distance have the form:

$$d_{bd}(reg_1, reg_2) = \begin{cases} \max(|\mathbf{c}_1 - \mathbf{c}_2| + \mathbf{o}_2 - \mathbf{o}_1) & \text{if } reg_2 \subseteq reg_1, \\ \|\max\{|\mathbf{c}_1 - \mathbf{c}_2| + \mathbf{o}_2 - \mathbf{o}_1, \mathbf{0}\}\|_2 & \text{else.} \end{cases}$$

Here,  $\max(\cdot)$  in the first line denotes the maximal value along all dimensions, while  $\max\{\cdot, \cdot\}$  in the second line applies element-wise to the two vectors or values.

The following proposition demonstrates that our definition of the boundary distance effectively captures the inclusion relationship between two regions in two key aspects, as illustrated in Figure 3: (i) it identifies whether one region is (exactly) contained within another, and (ii) it enhances discrimination in inclusion chains, as smaller regions tend to have larger boundary distances. This property is useful for distinguishing shallow children from deeper ones. It is worth noting that the proposition below applies to any regions, not only boxes or balls.

**Proposition 3.** For the boundary distance  $d_{bd}$  defined in Definition 2, the following properties hold:

1.  $d_{bd}(reg_1, reg_2) \leq 0$  if and only if  $reg_1 \subseteq reg_2$ . Moreover,  $d_{bd}(reg_1, reg_2) = 0$  if and only if  $reg_1$  is internally tangent to  $reg_2$ . That is,  $reg_1 \subseteq reg_2$ , and their boundaries intersect at some point.
2. If  $reg'_2 \subseteq reg_2 \subseteq reg_1$ , then

$$d_{bd}(reg_1, reg'_2) \leq d_{bd}(reg_1, reg_2).$$

## 4.2. Specific Constructions for Boxes or Balls

For specific geometric regions like balls and boxes, we can create specialized distance functions to measure the set-inclusion relationship based on their intrinsic geometric properties or established methods. Our framework accommodates these specialized metrics by allowing them to replace the general boundary distance function.

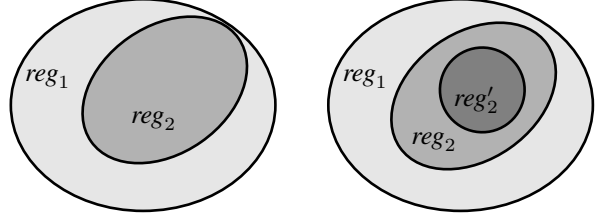


Figure 3. Illustration of internally tangent of item 1 (left) and item 2 (right) in Proposition 3.

1. **Volume-based distance for boxes:** Since the volume of a box can be computed as the product of its offsets along different dimensions, we can define a partial distance based on volume:

$$d_{vol}(reg_1, reg_2) = -\ln\left(\frac{\text{vol}(reg_1 \cap reg_2)}{\text{vol}(reg_2)}\right). \quad (5)$$

The negative logarithm ensures that the distance is non-negative and equals zero only when  $reg_2 \subseteq reg_1$ .

2. **hyperbolic distance for balls:** Yu et al. (2024) introduced a series of circular cones in hyperbolic space and defined a boundary distance based on the hyperbolic distance between the apex of these cones. By utilizing the natural mapping from balls to circular cones, we can derive a new boundary distance for balls as follows:

$$d_{bd}^{\text{cone}}(reg_1, reg_2) = \text{arcsinh}\left(\frac{\|\mathbf{c}_1 - \mathbf{c}_2\|_2 - r_1}{r_2}\right) + a, \quad (6)$$

where  $a = \text{arcsinh}(1)$ . See Appendix B for more details.

## 5. Training Strategy

**Energy** For a given pair  $(u, v)$ , we define their energy as:

$$E(u, v) = d_{bd}(reg_u, reg_v) + \lambda \cdot d_{\text{dep}}(reg_u, reg_v), \quad (7)$$

where  $\lambda$  is a weighting parameter that balances the contributions of the hyperbolic-like depth distance. This formulation ensures the simultaneous preservation of hyperbolic structural properties when needed, while maintaining the asymmetry characteristic of hierarchical relationships.

**Loss** To train our model, we employ a modified contrastive loss function as in (Yu et al., 2024):

$$\mathcal{L}(\gamma_1, \gamma_2) = \sum_{(u,v) \in P} \left( \max\{E(u, v), \gamma_1\} + \log\left(\sum_{(u,v') \in N} e^{\max\{\gamma_2 - d_{bd}(reg_u, reg_{v'}), 0\}}\right) \right), \quad (8)$$

where  $P$  and  $N$  denote positive and negative sample pairs, respectively. For **positive pairs**  $(u, v) \in P$ , the loss based on  $E(u, v)$  promotes both the containment of  $reg_v$  within  $reg_u$  (via the  $d_{bd}$  term) and their geometric similarity (via the  $d_{dep}$  term), whose contributions are controlled by the weight  $\lambda$  and the threshold  $\gamma_1$ . For **negative pairs**  $(u, v') \in N$ , since our primary goal is to push  $reg_{v'}$  outside of  $reg_u$ , it is sufficient to use the boundary distance  $d_{bd}(reg_u, reg_{v'})$  rather than the energy  $E(u, v')$ . A threshold  $\gamma_2$  is used to regulate how far  $reg_{v'}$  is pushed from  $reg_u$ .

Finally, we say that  $u$  is considered a parent of  $v$  (i.e.,  $u \prec v$ ) if  $E(u, v) \leq t$ , where  $t$  is a threshold that achieved the best performance on the evaluation set.

## 6. Evaluation

Our experiments aim to address two questions: **(1)** How effectively do our methods capture hierarchical relationships? and **(2)** Can they generalize to tasks involving more than hierarchies?

We evaluate hierarchical relationship modeling using transitive DAGs (Section 6.1). To assess generalization, we test on *ontologies* (see Appendix E for a formal definition), which extend pure hierarchies by incorporating logical operations like conjunction ( $\sqcap$ ) and existential quantifiers ( $\exists r.$ ). Ontologies contain “SubclassOf” ( $\sqsubseteq$ ) as a fundamental and ubiquitous relation, representing hierarchical structures. This makes ontologies ideal for evaluating beyond pure hierarchy modeling. Specifically, ontologies enable testing of: **(a)** Complex inferences tasks beyond transitive closure (Section 6.2); and **(b)** Link prediction across different, usually non-SubclassOf relations (Section 6.3).

### 6.1. Inferences over DAG

**Benchmark** Following (Yu et al., 2024), we evaluate our method on four real-world datasets consisting of Is-A relations: MCG (Wang et al., 2015; Wu et al., 2012), Hearst patterns (Hearst, 1992), the WordNet (Fellbaum, 1998) noun taxonomy, and its mammal subgraph. All models are trained exclusively on *basic edges*, which are edges not implied transitively by other edges in the graph. For validation and testing, we use the same sets as in (Yu et al., 2024), consisting of 5% of *non-basic (inferred)* edges, ensuring a fair comparison.

We exclude non-basic edges from training since they can be transitively derived from basic edges. Including them would artificially inflate performance metrics without properly evaluating the embeddings’ ability to capture hierarchical structures. For completeness, results for non-basic cases are provided in Appendix F.1.

**Baselines** We compare our method RegD with (i) hyperbolic approaches such as EntailmentCone (Ganea et al., 2018) and ShadowCone (Yu et al., 2024), which is the latest method with the state-of-the-art performance; (ii) region-based methods like OrderEmbedding (Bordes et al., 2013), and tBox (Boratto et al., 2021). We also compare with the ontology embedding methods, ELBE (Peng et al., 2022) and ELEM (Kulmanov et al., 2019), which can be considered as the baseline approaches embedding the DAG as boxes or balls, respectively. As in previous studies, the performance is evaluated using F1-scores.

**Results** The performance comparison across different DAGs is shown in Table 1. RegD achieved the best performance on all four datasets. Notably, the box variant consistently outperformed the ball variant in most cases, which might be because boxes contain more parameters than balls when embedded in the same dimensional space.

Interestingly, on the MCG and Hearst datasets, region-based methods outperformed hyperbolic methods. This may be attributed to the relatively low “hyperbolicity” of these datasets, as indicated by their larger  $\delta$ -hyperbolicity values in Table 2. In contrast, on the Noun dataset, despite its high  $\delta$ -hyperbolicity value, hyperbolic methods performed better. This discrepancy is likely due to the larger dataset size—containing over twice the number of nodes compared to the others—which leads to crowding effects in Euclidean space that limit the effectiveness of region-based methods. Nevertheless, our method performed consistently well in both cases, as it can adjust the hyperbolic component by setting different  $\lambda$  values in Equation (7).

### 6.2. Inference over Ontologies

**Benchmark** We utilize three normalized biomedical ontologies: GALEN (Rector et al., 1996), Gene Ontology (GO) (Ashburner et al., 2000), and Anatomy (Uberon) (Mungall et al., 2012). As in (Jackermeier et al., 2024), we use the entire ontology for training, and the complete set of inferred class subsumptions for testing. Those subsumptions can be regarded as partial order pairs  $u \prec v$ . Evaluation is performed using 1,000 subsumptions randomly sampled from the test set. Similar to inference over DAG, negative samples are generated by randomly replacing the child of each positive pair 10 times.

**Baselines** We focus on the most representative ontology embedding methods: ELBE (Peng et al., 2022) and ELEM (Kulmanov et al., 2019), as well as their enhanced versions incorporating RegD or  $\tau$ Box. Other hierarchy embedding methods are excluded from our tests due to their incompatibility with ontology embeddings. For example, OE and EntailmentCone utilizes cones as embedding objects, which cannot be directly integrated with ELBE or ELEM for on-

Table 1. F1 score (%) on Mammal, WordNet noun, MCG, and Hearst. Results with \* are coming from Yu et al. (2024).

Method	Mammal		Noun		MCG		Hearst		
	d=2	d=5	d=5	d=10	d=5	d=10	d=5	d=10	
$\tau$ Box	29.0	33.5	30.5	31.5	43.9	50.3	39.7	43.7	
OE	25.4	31.0	28.8	30.8	36.3	46.6	34.6	40.7	
ELBE (box baseline)	30.3	36.8	30.7	31.8	48.4	55.5	41.6	46.8	
ELEM (ball baseline)	27.7	28.8	28.6	29.5	35.7	38.6	34.6	36.7	
EntailmentCone*	54.4	56.3	29.2	32.1	25.3	25.5	22.6	23.7	
ShadowCone*	(Umbral-half-space)	57.7	69.4	45.2	52.2	36.8	40.1	32.8	32.6
	(Penumbrahalf-space)	52.8	67.8	44.6	51.7	35.0	37.6	26.8	28.4
RegD	(box)	<b>64.9</b>	<b>74.4</b>	53.8	51.3	<b>50.7</b>	<b>58.5</b>	<b>42.8</b>	<b>49.6</b>
	(ball)	62.7	71.8	<b>58.4</b>	<b>59.1</b>	44.9	46.8	37.7	37.7

Table 2. Summary of Graph Metrics, where  $\delta$ -Hyp (max/mean) indicates the  $\delta$ -Hyperbolicity (see Appendix D). Lower values suggest more “hyperbolic” structures, and a value of 0 indicates a tree.

	Mammal	Noun	MCG	Hearst
<b>Nodes</b>	1,179	82,114	22,665	35,545
<b>Edges</b>	1,176	84,363	38,288	42,423
<b><math>\delta</math>-Hyp</b>	0.0 / 0.0	4.5 / 0.512	2.0 / 0.316	2.5 / 0.426

tology tasks. Details of the integration are provided in Appendix F.2.

**Results** The results are summarized in Tables 3. We can see that RegD yields consistent improvements across all ontologies for inferencing tasks. Specifically, it gains—an F1 score increase of more than 45% with ELBE method on the ANATOMY ontology. Conversely, the  $\tau$ Box plugin consistently reduces performance across nearly all test cases, underscoring its limited applicability to tasks involving more than hierarchies.

### 6.3. Link Prediction over Ontologies

We use the same baselines and datasets as described in Section 6.2. However, in this prediction task, we partition the original ontologies directly into 80% for training, 10% for validation, and 10% for testing as in (Jackermeier et al., 2024). For the link prediction task, we focus on specific parts of the validation and testing sets, represented as  $\exists r.B \prec ?A$ , where  $A$  and  $B$  are concept names and  $r$  is a role. This setup is equivalent to link prediction tasks  $(?A, r, B)$  in knowledge graphs if we regard  $A$ ,  $B$ , and  $r$  as the head entity, tail entity, and relation, respectively.

Table 3. F1 score (%) for the inference task on ontologies.

Dataset	Dim	GALEN	GO	ANATOMY
ELBE		20.7	36.9	43.1
+ $\tau$ Box	d=5	20.8	32.2	42.2
+ RegD		<b>25.2</b>	<b>50.0</b>	<b>58.7</b>
ELBE		21.2	42.4	43.0
+ $\tau$ Box	d=10	20.7	34.7	47.2
+ RegD		<b>25.8</b>	<b>50.5</b>	<b>62.5</b>
ELEM		16.9	23.5	34.6
+ RegD	d=5	<b>19.2</b>	<b>36.4</b>	<b>52.5</b>
ELEM		17.3	27.4	38.7
+ RegD	d=10	<b>18.8</b>	<b>40.0</b>	<b>55.5</b>

**Results** Table 3 summarizes the results. RegD shows mixed results: while it generally improves performance, it decreases scores on the GALEN ontology and ANATOMY ontology with ELEM. This degradation likely occurs in challenging prediction cases where all methods perform poorly. Nevertheless, RegD achieves significant improvements in other cases, notably increasing F1 score by 77.6% with ELBE on the ANATOMY ontology. In contrast, the  $\tau$ Box plugin consistently reduces performance across almost all test cases.

## 7. Conclusion

We introduced a framework RegD for low-dimensional embeddings of hierarchies, leveraging two distance metrics between regions. Our method, applicable to regions in the Euclidean space, demonstrates versatility and has the potential for a wide range of tasks involving data beyond hierarchies. Additionally, we showed that our approach achieves comparable embedding performance to hyperbolic methods while



Table 4. F1 score (%) for the prediction task on ontologies.

Dataset	Dim	GALEN	GO	ANATOMY
ELBE		<b>21.0</b>	32.8	25.1
+ $\tau$ Box	d=5	18.4	24.0	25.6
+ RegD		20.6	<b>37.1</b>	<b>41.4</b>
ELBE		<b>24.2</b>	37.9	25.5
+ $\tau$ Box	d=10	19.5	29.3	22.9
+ RegD		21.0	<b>44.1</b>	<b>45.3</b>
ELEM		16.7	54.5	<b>23.1</b>
+ RegD	d=5	<b>16.8</b>	<b>60.3</b>	21.7
ELEM		16.6	54.2	<b>26.0</b>
+ RegD	d=10	<b>18.0</b>	<b>61.4</b>	21.9

being significantly simpler to implement.

For future work, we aim to extend the applicability of our methods to diverse geometric regions, tailoring their geometric properties to the specific requirements of different tasks. Moreover, we plan to explore additional applications beyond hierarchical structures, including integrating our framework with language models, as in (He et al., 2024b).

## References

- Abboud, R., Ceylan, İ. İ., Lukasiewicz, T., and Salvatori, T. Boxe: A box embedding model for knowledge base completion. In Larochelle, H., Ranzato, M., Hadsell, R., Balcan, M., and Lin, H. (eds.), *Advances in Neural Information Processing Systems 33: Annual Conference on Neural Information Processing Systems 2020, NeurIPS 2020, December 6-12, 2020, virtual*, 2020. URL [https://proceedings.neurips.cc/paper/2020/hash/1c0b06977fc30100000000000000000-Abstract.html](https://proceedings.neurips.cc/paper/2020/hash/1c0b06977fc301000000000000000000-Abstract.html).
- Ashburner, M., Ball, C. A., Blake, J. A., Botstein, D., Butler, H., Cherry, J. M., Davis, A. P., Dolinski, K., Dwight, S. S., Eppig, J. T., et al. Gene ontology: tool for the unification of biology. *Nature genetics*, 25(1):25–29, 2000.
- Baader, F. and Gil, O. F. Extending the description logic EL with threshold concepts induced by concept measures. *Artif. Intell.*, 326:104034, 2024. doi: 10.1016/J.ARTINT.2023.104034. URL <https://doi.org/10.1016/j.artint.2023.104034>.
- Baader, F., Horrocks, I., Lutz, C., and Sattler, U. *An Introduction to Description Logic*. Cambridge University Press, 2017. ISBN 978-0-521-69542-8. URL <http://www.cambridge.org/de/academic/subj>.
- Balazevic, I., Allen, C., and Hospedales, T. M. Multi-relational poincaré graph embeddings. In Wallach, H. M., Larochelle, H., Beygelzimer, A., d’Alché-Buc, F., Fox, E. B., and Garnett, R. (eds.), *Advances in Neural Information Processing Systems 32: Annual Conference on Neural Information Processing Systems 2019, NeurIPS 2019, December 8-14, 2019, Vancouver, BC, Canada*, pp. 4465–4475, 2019. URL <https://proceedings.neurips.cc/paper/2019/hash/f8>.
- Béginneul, G. and Ganea, O. Riemannian adaptive optimization methods. In *7th International Conference on Learning Representations, ICLR 2019, New Orleans, LA, USA, May 6-9, 2019*. OpenReview.net, 2019. URL <https://openreview.net/forum?id=rleiqi09K7>.
- Boratko, M., Zhang, D., Monath, N., Vilnis, L., Clarkson, K. L., and McCallum, A. Capacity and bias of learned geometric embeddings for directed graphs. In Ranzato, M., Beygelzimer, A., Dauphin, Y. N., Liang, P., and Vaughan, J. W. (eds.), *Advances in Neural Information Processing Systems 34: Annual Conference on Neural Information Processing Systems 2021, NeurIPS 2021, December 6-14, 2021, virtual*, pp. 16423–16436, 2021. URL <https://proceedings.neurips.cc/paper/2021/hash/88>.
- Bordes, A., Usunier, N., García-Durán, A., Weston, J., and Yakhnenko, O. Translating embeddings for modeling multi-relational data. In Burges, C. J. C., Bottou, L., Ghahramani, Z., and Weinberger, K. Q. (eds.), *Advances in Neural Information Processing Systems 26: 27th Annual Conference on Neural Information Processing Systems 2013. Proceedings of a meeting held December 5-8, 2013, Lake Tahoe, Nevada, United States*, pp. 2787–2795, 2013. URL <https://proceedings.neurips.cc/paper/2013/hash/1c>.
- Chen, J., Mashkova, O., Zhapa-Camacho, F., Hoehn-dorn, R., He, Y., and Horrocks, I. Ontology embedding: A survey of methods, applications and resources. *CoRR*, abs/2406.10964, 2024. doi: 10.48550/ARXIV.2406.10964. URL <https://doi.org/10.48550/arXiv.2406.10964>.
- Dasgupta, S. S., Boratko, M., Zhang, D., Vilnis, L., Li, X., and McCallum, A. Improving local identifiability in probabilistic box embeddings. In Larochelle, H., Ranzato, M., Hadsell, R., Balcan, M., and Lin, H. (eds.), *Advances in Neural Information Processing Systems 33: Annual Conference on Neural Information Processing Systems 2020, NeurIPS 2020, December 6-12, 2020, virtual*, 2020. URL <https://proceedings.neurips.cc/paper/2020/hash/01>.
- Fellbaum, C. Wordnet: An electronic lexical database. *MIT Press google schola*, 2:678–686, 1998.
- Ganea, O., Béginneul, G., and Hofmann, T. Hyperbolic entailment cones for learning hierarchical embeddings.

- In Dy, J. G. and Krause, A. (eds.), *Proceedings of the 35th International Conference on Machine Learning, ICML 2018, Stockholmsmässan, Stockholm, Sweden, July 10-15, 2018*, volume 80 of *Proceedings of Machine Learning Research*, pp. 1632–1641. PMLR, 2018. URL <http://proceedings.mlr.press/v80/ganea18a.html>.
- Gromov, M. Hyperbolic groups. *Essays in Group Theory, pages/Springer-Verlag*, 1987.
- He, Y., Chen, J., Dong, H., Horrocks, I., Allocca, C., Kim, T., and Sapkota, B. Deeponto: A python package for ontology engineering with deep learning. *Semantic Web*, 15 (5):1991–2004, 2024a. doi: 10.3233/SW-243568. URL <https://doi.org/10.3233/SW-243568>.
- He, Y., Yuan, Z., Chen, J., and Horrocks, I. Language models as hierarchy encoders. In *Advances in Neural Information Processing Systems (NeurIPS)*, 2024b. Accepted.
- Hearst, M. A. Automatic acquisition of hyponyms from large text corpora. In *14th International Conference on Computational Linguistics, COLING 1992, Nantes, France, August 23-28, 1992*, pp. 539–545, 1992. URL <https://aclanthology.org/C92-2082/>.
- Jackermeier, M., Chen, J., and Horrocks, I. Dual box embeddings for the description logic  $el^{++}$ . In Chua, T., Ngo, C., Kumar, R., Lauw, H. W., and Lee, R. K. (eds.), *Proceedings of the ACM on Web Conference 2024, WWW 2024, Singapore, May 13-17, 2024*, pp. 2250–2258. ACM, 2024. doi: 10.1145/3589334.3645648. URL <https://doi.org/10.1145/3589334.3645648>.
- Kulmanov, M., Liu-Wei, W., Yan, Y., and Hoehndorf, R. EL embeddings: Geometric construction of models for the description logic  $EL^{++}$ . In *Proceedings of the Twenty-Eighth International Joint Conference on Artificial Intelligence*, pp. 6103–6109. International Joint Conferences on Artificial Intelligence Organization, 2019. ISBN 978-0-9992411-4-1. doi: 10.24963/ijcai.2019/845. URL <https://www.ijcai.org/proceedings/2019/845>.
- Lee, J. *Introduction to Smooth Manifolds*. Graduate Texts in Mathematics. Springer Science & Business Media, 2013. ISBN 978-0-387-21752-9.
- Lee, J. M. *Riemannian manifolds: an introduction to curvature*, volume 176. Springer Science & Business Media, 2006.
- Mikolov, T., Chen, K., Corrado, G., and Dean, J. Efficient estimation of word representations in vector space. In Bengio, Y. and LeCun, Y. (eds.), *1st International Conference on Learning Representations, ICLR 2013, Scottsdale, Arizona, USA, May 2-4, 2013, Workshop Track Proceedings*, 2013. URL <http://arxiv.org/abs/1301.3781>.
- Mungall, C. J., Torniai, C., Gkoutos, G. V., Lewis, S. E., and Haendel, M. A. Uberon, an integrative multi-species anatomy ontology. *Genome biology*, 13:1–20, 2012.
- Nickel, M. and Kiela, D. Poincaré embeddings for learning hierarchical representations. In Guyon, I., von Luxburg, U., Bengio, S., Wallach, H. M., Fergus, R., Vishwanathan, S. V. N., and Garnett, R. (eds.), *Advances in Neural Information Processing Systems 30: Annual Conference on Neural Information Processing Systems 2017, December 4-9, 2017, Long Beach, CA, USA*, pp. 6338–6347, 2017. URL <https://proceedings.neurips.cc/paper/2017/hash/59>
- Peng, X., Tang, Z., Kulmanov, M., Niu, K., and Hoehndorf, R. Description logic  $EL^{++}$  embeddings with intersectional closure, 2022. URL <http://arxiv.org/abs/2202.14018>.
- Pennington, J., Socher, R., and Manning, C. D. Glove: Global vectors for word representation. In Moschitti, A., Pang, B., and Daelemans, W. (eds.), *Proceedings of the 2014 Conference on Empirical Methods in Natural Language Processing, EMNLP 2014, October 25-29, 2014, Doha, Qatar; A meeting of SIG-DAT, a Special Interest Group of the ACL*, pp. 1532–1543. ACL, 2014. doi: 10.3115/V1/D14-1162. URL <https://doi.org/10.3115/v1/d14-1162>.
- Rector, A. L., Rogers, J. E., and Pole, P. The galen high level ontology. In *Medical Informatics Europe’96*, pp. 174–178. IOS Press, 1996.
- Shen, J. and Han, J. *Automated Taxonomy Discovery and Exploration*. Synthesis Lectures on Data Mining and Knowledge Discovery. Springer, 2022. ISBN 978-3-031-11404-5. doi: 10.1007/978-3-031-11405-2. URL <https://doi.org/10.1007/978-3-031-11405-2>.
- Shi, J., Dong, H., Chen, J., Wu, Z., and Horrocks, I. Taxonomy completion via implicit concept insertion. In Chua, T., Ngo, C., Kumar, R., Lauw, H. W., and Lee, R. K. (eds.), *Proceedings of the ACM on Web Conference 2024, WWW 2024, Singapore, May 13-17, 2024*, pp. 2159–2169. ACM, 2024. doi: 10.1145/3589334.3645584. URL <https://doi.org/10.1145/3589334.3645584>.
- Sun, Z., Deng, Z., Nie, J., and Tang, J. Rotate: Knowledge graph embedding by relational rotation in complex space. In *7th International Conference on Learning Representations, ICLR 2019, New Orleans*,

LA, USA, May 6-9, 2019. OpenReview.net, 2019. URL <https://openreview.net/forum?id=HkgEQnRqYQ>.

Suzuki, R., Takahama, R., and Onoda, S. Hyperbolic disk embeddings for directed acyclic graphs. In Chaudhuri, K. and Salakhutdinov, R. (eds.), *Proceedings of the 36th International Conference on Machine Learning, ICML 2019, 9-15 June 2019, Long Beach, California, USA*, volume 97 of *Proceedings of Machine Learning Research*, pp. 6066–6075. PMLR, 2019. URL <http://proceedings.mlr.press/v97/suzuki19a.html>.

Vendrov, I., Kiros, R., Fidler, S., and Urtasun, R. Order-embeddings of images and language. In Bengio, Y. and LeCun, Y. (eds.), *4th International Conference on Learning Representations, ICLR 2016, San Juan, Puerto Rico, May 2-4, 2016, Conference Track Proceedings, 2016*. URL <http://arxiv.org/abs/1511.06361>.

Vilnis, L., Li, X., Murty, S., and McCallum, A. Probabilistic embedding of knowledge graphs with box lattice measures. In Gurevych, I. and Miyao, Y. (eds.), *Proceedings of the 56th Annual Meeting of the Association for Computational Linguistics, ACL 2018, Melbourne, Australia, July 15-20, 2018, Volume 1: Long Papers*, pp. 263–272. Association for Computational Linguistics, 2018. doi: 10.18653/V1/P18-1025. URL <https://aclanthology.org/P18-1025/>.

Wang, Z., Wang, H., Wen, J., and Xiao, Y. An inference approach to basic level of categorization. In Bailey, J., Moffat, A., Aggarwal, C. C., de Rijke, M., Kumar, R., Murdock, V., Sellis, T. K., and Yu, J. X. (eds.), *Proceedings of the 24th ACM International Conference on Information and Knowledge Management, CIKM 2015, Melbourne, VIC, Australia, October 19 - 23, 2015*, pp. 653–662. ACM, 2015. doi: 10.1145/2806416.2806533. URL <https://doi.org/10.1145/2806416.2806533>.

Wu, W., Li, H., Wang, H., and Zhu, K. Q. Probase: a probabilistic taxonomy for text understanding. In Candan, K. S., Chen, Y., Snodgrass, R. T., Gravano, L., and Fuxman, A. (eds.), *Proceedings of the ACM SIGMOD International Conference on Management of Data, SIGMOD 2012, Scottsdale, AZ, USA, May 20-24, 2012*, pp. 481–492. ACM, 2012. doi: 10.1145/2213836.2213891. URL <https://doi.org/10.1145/2213836.2213891>.

Yu, T., Liu, T. J. B., Tseng, A., and Sa, C. D. Shadow cones: A generalized framework for partial order embeddings. In *The Twelfth International Conference on Learning Representations, ICLR 2024, Vienna, Austria, May 7-11, 2024*. OpenReview.net, 2024. URL <https://openreview.net/forum?id=zbKcFZ6Dbp>.

## A. Proofs

### A.1. Theorem 1

*Proof of Theorem 1.* We begin by proving the result for balls and addressing each item as follows:

1. Assume  $reg_1 = ball(\mathbf{c}_1, r_1)$  and  $reg_2 = ball(\mathbf{c}_2, r_2)$ . For any ball  $ball(\mathbf{c}', r') \subseteq ball(\mathbf{c}_2, r_2)$  with  $r' \leq 0.5 \cdot r_1$ , we must have:

$$\sum_i |\mathbf{c}_i - \mathbf{c}'|^p + |r - r'|^p > (0.5 \cdot r_1)^p.$$

Therefore, we have:

$$d_{\text{dep}}(reg_1, ball(\mathbf{c}', r')) = \frac{\sum_i |\mathbf{c}_i - \mathbf{c}'|^p + |r - r'|^p}{f(ball)f(ball')} > \frac{(\frac{1}{2}r_1)^p}{f(ball)f(ball')}.$$

Thus, when:

$$f(ball(\mathbf{c}', r')) < \epsilon := \frac{f(ball)f(ball')[d_{\text{dep}}(reg_1, reg_2) + N]}{(\frac{1}{2}r_1)^p},$$

we can guarantee that  $d_{\text{dep}}(reg_1, ball(\mathbf{c}', r')) > d_{\text{dep}}(reg_1, reg_2) + N$ .

Note that by our assumption, we have:

$$\lim_{reg \rightarrow \emptyset} f(reg) = 0.$$

Therefore, there exists a  $\delta > 0$  such that when  $r < \delta$ , we have  $f(reg) \leq \epsilon$  for  $reg = ball(\mathbf{c}, r)$ . In conclusion,  $r_0 = \min\{\delta, 0.5 \cdot r_1\}$  satisfies the required condition.

2. Assume  $reg = ball(\mathbf{c}, r)$ . For any  $n, M > 0$ , we can select  $n$  distinct vectors  $\mathbf{c}_1, \dots, \mathbf{c}_n \in ball(\mathbf{c}, 0.5 \cdot r)$  such that:

$$\|\mathbf{c}_i - \mathbf{c}_j\|_p^p > \delta > 0 \quad \text{for some } \delta > 0.$$

Similarly to item 1, we can choose  $\delta$  small enough such that for any ball  $ball(\mathbf{c}_i, r_i)$  with  $r_i < \delta$ , we have:

$$f(ball(\mathbf{c}_i, r_i)) < \left(\frac{\delta}{M}\right)^{0.5}.$$

Thus, we obtain:

$$d_{\text{dep}}(ball(\mathbf{c}_i, r_i), ball(\mathbf{c}_j, r_j)) > \frac{\delta}{f(ball(\mathbf{c}_i, r_i))f(ball(\mathbf{c}_j, r_j))} \geq M.$$

This concludes the proof of item 2.

The proof for the case of boxes follows the same reasoning, with the radius  $r$  replaced by the offset  $\mathbf{o}$  or its norm  $\|\mathbf{o}\|$ .  $\square$

### A.2. Proposition 1

*Proof of Proposition 1.* Recall that when the curvature is  $-1$ , the distance in the hyperbolic space (half-plane model) is given by:

$$d_{\mathbb{H}}(\mathbf{x}, \mathbf{y}) = \text{arcosh} \left( 1 + \frac{\|\mathbf{x} - \mathbf{y}\|^2}{2\mathbf{x}_n \mathbf{y}_n} \right).$$

The distance induced by the function  $F$  is of the form:

$$d_{\mathbb{B}^n}^{\#}(ball(\mathbf{c}, r), ball'(\mathbf{c}', r')) = \text{arcosh} \left( 1 + \frac{\|\mathbf{c} - \mathbf{c}'\|^2 + (r - r')^2}{2rr'} \right).$$

This coincides with the depth distance in Example 1 when  $p = 2$ ,  $g(x) = \text{arcosh}(x + 1)$ , and  $h(ball) = \sqrt{2}$ . This completes the proof.  $\square$



### A.3. Proposition 2

*Proof of Proposition 2.* This proposition follows directly from Proposition 1. The function  $g(x) = \operatorname{arcosh}(x + 1)$  is an increasing bijection from  $\mathbb{R}_{\geq 0}$  to  $\mathbb{R}_{\geq 0}$ . Thus, for any  $x, x' \geq 0$ , we have:

$$x \leq x' \iff g^{-1}(x) \leq g^{-1}(x').$$

By the assumption of this proposition,  $d_{\text{dep}}(\cdot, \cdot) = g^{-1}(d_{\mathbb{H}^n}(\cdot, \cdot))$ . Therefore, for any points  $\mathbf{x}_1, \mathbf{x}_2, \mathbf{x}_3, \mathbf{x}_4 \in \mathbb{H}^n$ , we have:

$$d_{\mathbb{H}^n}(\mathbf{x}_1, \mathbf{x}_2) < d_{\mathbb{H}^n}(\mathbf{x}_3, \mathbf{x}_4)$$

if and only if

$$d_{\text{dep}}(F^{-1}(\mathbf{x}_1), F^{-1}(\mathbf{x}_2)) < d_{\text{dep}}(F^{-1}(\mathbf{x}_3), F^{-1}(\mathbf{x}_4)).$$

□

### A.4. Proposition 3

*Proof of Proposition 3.* We prove each item one-by-one:

1. By definition, we have  $d_{\text{bd}}(\text{reg}_1, \text{reg}_2) \leq 0$  if and only if  $\text{reg}_1 \subseteq \text{reg}_2$ . Next, we focus on the case  $d_{\text{bd}}(\text{reg}_1, \text{reg}_2) = 0$ .

Note that if  $d_{\text{bd}}(\text{reg}_1, \text{reg}_2) = 0$ , we must have  $\text{reg}_1 \subseteq \text{reg}_2$ . Otherwise, we have

$$d_{\text{bd}}(\text{reg}_1, \text{reg}_2) = \max_{\mathbf{x}_2 \in \text{reg}_2 \setminus \text{reg}_1} \{d(\text{reg}_1, \mathbf{x}_2)\} = 0$$

Therefore, for any  $\mathbf{x}_2 \in \text{reg}_2$ , we have  $d(\text{reg}_1, \mathbf{x}_2) = 0$ , therefore  $\mathbf{x}_2 \subseteq \text{reg}_1$  (assuming  $\text{reg}_1$  is a closed set). Contradiction!

Since  $\text{reg}_1 \subseteq \text{reg}_2$ , we have

$$d_{\text{bd}}(\text{reg}_1, \text{reg}_2) = \max_{\mathbf{x}_2 \in \text{reg}_2} \{-d(\text{reg}_1^c, \mathbf{x}_2)\} = 0.$$

Therefore, there must exist  $\mathbf{x}_2 \in \text{reg}_2$  such that  $d(\text{reg}_1^c, \mathbf{x}_2) = 0$ , and thus  $\mathbf{x}_2 \in \text{reg}_1^c$ . Since we have  $\mathbf{x}_2 \subseteq \text{reg}_2 \subseteq \text{reg}_1$ , therefore,  $\mathbf{x}_2 \in \partial(\text{reg}_1)$ . Similarly, since  $\mathbf{x}_2 \subseteq \text{reg}_1^c \subseteq \text{reg}_2^c$  and  $\mathbf{x}_2 \in \text{reg}_2$ , we also have  $\mathbf{x}_2 \in \partial(\text{reg}_2)$ . This finishes the proof of the first case.

2. By assumption, we have

$$d_{\text{bd}}(\text{reg}_1, \text{reg}_2) = \max_{\mathbf{x}_2 \in \text{reg}_2} \{-d(\text{reg}_1^c, \mathbf{x}_2)\}, \quad d_{\text{bd}}(\text{reg}_1, \text{reg}'_2) = \max_{\mathbf{x}_2 \in \text{reg}'_2} \{-d(\text{reg}_1^c, \mathbf{x}_2)\}.$$

Since  $\text{reg}'_2 \subseteq \text{reg}_2$ , of course we have

$$d_{\text{bd}}(\text{reg}_1, \text{reg}'_2) \leq d_{\text{bd}}(\text{reg}_1, \text{reg}_2).$$

This finishes the proof of the second case.

□

## B. Hyperbolic Boundary Distance for Balls

A ball in  $\mathbb{R}^n$  can be mapped to a cone in the upper half-space  $\mathbb{R}^n \times \mathbb{R}_{\geq 0}$  via a mapping  $G$ . This transformation is illustrated in Figure 4 for the case  $n = 1$ , where a ball  $\text{ball}(0, 1)$  is mapped to a cone with apex  $(0, 1) \in \mathbb{R} \times \mathbb{R}_{\geq 0}$ . Note that the height of the cone corresponds to the radius of the underlying ball. The upper half-space can be interpreted as the Poincaré half-plane model of hyperbolic space.

Formally, we are considering a cone with a base as a ball  $\text{ball}(\mathbf{c}, r)$  and a height  $k > 0$ , which can be defined as:

$$\text{Cone}(\text{ball}(\mathbf{c}, r), k) = \{(1-t)\mathbf{x} + t(\mathbf{c} + k\mathbf{e}_{n+1}) : \mathbf{x} \in \text{ball}(\mathbf{c}, r), t \in [0, 1]\}, \quad \text{where } \mathbf{e}_{n+1} = (0, \dots, 0, 1) \in \mathbb{R}^{n+1}.$$

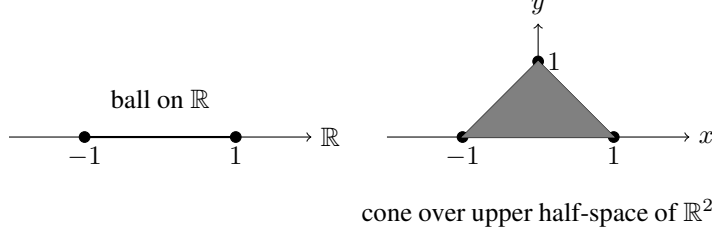


Figure 4. Mapping from balls to cones in the case of dimension 1.

The mapping  $G$  is defined by:

$$G(\text{ball}(\mathbf{c}, r)) = \text{Cone}(\text{ball}(\mathbf{c}, r), r).$$

The boundary distance between two cones in the Poincaré half-plane model (as shown on the right of Figure 4) can be defined as:

$$d_{\text{bd}}^{\text{cone}}(\text{Cone}_1, \text{Cone}_2) := \chi \cdot \min d_{\mathbb{H}}(\partial(\text{Cone}_1), \text{Apex}(\text{Cone}_1)),$$

where  $\chi = -1$  if  $\text{Cone}_2 \subseteq \text{Cone}_1$ , and  $\chi = 1$  otherwise.  $\partial(\text{Cone}_1)$  denotes the boundary of  $\text{Cone}_1$ , and  $\text{Apex}(\text{Cone}_1)$  is the apex of  $\text{Cone}_1$ .

Assuming the curvature is fixed at  $-1$  (i.e.,  $k = 1$ ), we specialize Theorem 4.2 from Yu et al. (2024) by imposing the condition  $\sinh(\sqrt{k}r) = 1$ , from which we derive:

$$d_{\text{bd}}^{\text{cone}}(\text{Cone}_1(\text{ball}(\mathbf{c}_1, r_1), r_1), \text{Cone}_2(\text{ball}(\mathbf{c}_2, r_2), r_2)) = \text{arcsinh}\left(\frac{\|\mathbf{c}_1 - \mathbf{c}_2\| - r_1}{r_2}\right) + \text{arcsinh}(1),$$

where  $\mathbf{c}_i$  and  $r_i$  are the center and radius of the underlying balls corresponding to the cones.

This distance can be extended back to the context of balls, allowing the definition of a boundary distance between balls as:

$$d_{\text{bd}}^{\text{cone}}(\text{ball}_1(\mathbf{c}_1, r_1), \text{ball}_2(\mathbf{c}_2, r_2)) = \text{arcsinh}\left(\frac{\|\mathbf{c}_1 - \mathbf{c}_2\| - r_1}{r_2}\right) + \text{arcsinh}(1).$$

### C. Poincare Ball Models

There exist multiple models  $\mathbb{H}$  that are isometric to each other. This work uses two such models, the Poincaré ball and the Poincaré half-space:

The **Poincaré ball** is given by

$$B^n = \{x \in \mathbb{R}^n : \|x\| < 1/\sqrt{k}\}.$$

Distances on  $B^n$  are defined as

$$d_{\mathbb{H}}(x, y) = \frac{1}{\sqrt{k}} \text{arccosh}\left(1 + \frac{2k\|x - y\|^2}{(1 - k\|x\|^2)(1 - k\|y\|^2)}\right).$$

### D. $\delta$ -Hyperbolicity

In the study of metric spaces, a space is said to be  $\delta$ -hyperbolic if it satisfies a particular property related to the triangle inequality. The concept of  $\delta$ -hyperbolicity was introduced by M. Gromov (Gromov, 1987) to capture the notion of negative curvature in a metric space.

**Definition D.1** ( $\delta$ -Hyperbolicity). Let  $(X, d)$  be a metric space, where  $d$  is a distance function between points in  $x$ . For any three points  $x, y, z \in X$ , the *Gromov product* is defined by:

$$(y \cdot z)_x = \frac{1}{2}(d(x, y) + d(x, z) - d(y, z))$$

The space is called  $\delta$ -hyperbolic if there exists a constant  $\delta \geq 0$  such that for all points  $x, y, z, w \in X$ :

$$(y \cdot z)_x \geq \min\{(y \cdot w)_x, (w \cdot z)_x\} - \delta$$

Generally, a  $\delta$ -hyperbolic space approximates a hyperbolic geometry when  $\delta$  is small, and it approximates Euclidean geometry as  $\delta$  grows large. Moreover,  $\delta$ -hyperbolicity can also be applied to discrete spaces such as graphs, with the distance  $d(x, y)$  is the shortest path distance between two vertices  $x$  and  $y$ . In this context,  $\delta$ -hyperbolicity helps capture the "thickness" of the graph's structure and can be used to analyze its intrinsic geometry.

**Approximate Computing Process of  $\delta$ -Hyperbolicity**  $\delta$ -Hyperbolicity can be computed approximately by randomly sampling a subset of quadruples. Formally, by sampling  $N$  quadruples  $(x, y, z, w)$  from a set  $S$ , the approximate value of  $\delta$ -hyperbolicity can be computed as

$$\delta_{\text{app}} = \max \{ \min \{ (y \cdot w)_x, (w \cdot z)_x \} - (y \cdot z)_x \mid (x, y, z, w) \in S \}.$$

To provide a more robust estimate, we also compute the mean value of the  $\delta$ -hyperbolicity across all samples. This allows us to capture both the maximal influence of local behavior and the overall average property of the space. For example, in Table 2, we approximate the  $\delta$ -hyperbolicity by sampling 50,000 quadruples and report both the maximum and the mean of the sampling results to offer a comprehensive understanding of the space's geometric characteristics.

## E. Ontologies

Ontologies use sets of statements (axioms) about concepts (unary predicates) and roles (binary predicates) for knowledge representation and reasoning. We focus on  $\mathcal{EL}$ -ontologies, which strike a good balance between expressivity and reasoning efficiency, making them widely applicable (Baader & Gil, 2024).

Let  $N_C = \{A, B, \dots\}$ ,  $N_R = \{r, t, \dots\}$ , and  $N_I = \{a, b, \dots\}$  be pairwise disjoint sets of *concept names* (also called *atomic concepts*), *role names*, and *individual names*, respectively.  $\mathcal{EL}$ -concepts are recursively defined from atomic concepts, roles, and individuals as follows:

$$\top \mid \perp \mid A \mid C \sqcap D \mid \exists r.C \mid \{a\}$$

An  $\mathcal{EL}^{++}$ -ontology is a finite set of TBox axioms of the form

$$C \sqsubseteq D.$$

Note that here  $\sqsubseteq$  denotes "Subclass Of," which is a transitive relation that can be considered a partial order  $\prec$  by rewriting it as:

$$C \sqsubseteq D \Leftrightarrow D \prec C.$$

**Example 4.** From atomic concepts *Father*, *Child*, *Male*, ... and the role *hasParent*, we can construct a small family ontology consisting of two TBox axioms:

$$\text{Father} \sqsubseteq \text{Male} \sqcap \text{Parent}, \quad \text{Child} \sqsubseteq \exists \text{hasParent.Father}.$$

An *interpretation*  $\mathcal{I} = (\Delta^{\mathcal{I}}, \cdot^{\mathcal{I}})$  consists of a non-empty set  $\Delta^{\mathcal{I}}$  and a function  $\cdot^{\mathcal{I}}$  that maps each  $A \in N_C$  to  $A^{\mathcal{I}} \subseteq \Delta^{\mathcal{I}}$ , and each  $r \in N_R$  to  $r^{\mathcal{I}} \subseteq \Delta^{\mathcal{I}} \times \Delta^{\mathcal{I}}$ , where  $\perp^{\mathcal{I}} = \emptyset$  and  $\top^{\mathcal{I}} = \Delta^{\mathcal{I}}$ . The function  $\cdot^{\mathcal{I}}$  is extended to any  $\mathcal{EL}$ -concepts as follows:

$$(C \sqcap D)^{\mathcal{I}} = C^{\mathcal{I}} \cap D^{\mathcal{I}}, \tag{9}$$

$$(\exists r.C)^{\mathcal{I}} = \{a \in \Delta^{\mathcal{I}} \mid \exists b \in C^{\mathcal{I}} : (a, b) \in r^{\mathcal{I}}\}. \tag{10}$$

An interpretation  $\mathcal{I}$  satisfies a TBox axiom  $X \sqsubseteq Y$  if  $X^{\mathcal{I}} \subseteq Y^{\mathcal{I}}$  for  $X$  and  $Y$  being either two concepts or two role names, or  $X$  being a role chain and  $Y$  being a role name. An ontology  $\mathcal{O}$  entails an axiom  $C \sqsubseteq D$ , written

$$\mathcal{O} \models C \sqsubseteq D \quad (\text{i.e., } \mathcal{O} \models D \prec C),$$

if  $C \sqsubseteq D$  is satisfied by all models of  $\mathcal{O}$ . Ontologies can infer much more complex patterns than the transitive closure.

**Example 5.** In an ontology, suppose that in a group  $X$ , all members are both a man and a parent. That is,  $X \sqsubseteq \text{man}$  and  $X \sqsubseteq \text{parent}$  in the ontology. Moreover, man and parent together imply father (formally,  $\text{man} \sqcap \text{parent} \sqsubseteq \text{father}$  in the ontology). From this, we can infer that the group  $X$  is a father, which is not derivable from the transitive closure.

Table 5. F1 score (%) on Mammal, WordNet noun, MCG, and Hearst with best numbers **bolded**.

		Options		Mammal		Noun		MCG		Hearst	
region	$\lambda$	$p$	boundary distance	d=2	d=5	d=5	d=10	d=5	d=10	d=5	d=10
Box	0	-	$d_{bd}$	39.4	42.8	34.6	34.6	<u>49.9</u>	56.6	<u>41.6</u>	<u>44.7</u>
			$d_{vol}$	31.7	38.1	30.8	31.9	48.6	<b>58.5</b>	<b>42.8</b>	<b>49.6</b>
	> 0	1	$d_{bd}$	<b>64.9</b>	<b>74.4</b>	53.8	51.3	43.7	45.0	35.6	38.8
			$d_{vol}$	45.6	54.3	30.4	33.4	30.9	39.9	32.6	38.8
		2	$d_{bd}$	56.1	62.2	50.3	47.4	<b>50.7</b>	<u>57.4</u>	40.6	44.6
			$d_{vol}$	39.7	47.9	30.6	31.6	48.5	<u>56.7</u>	37.8	43.8
Ball	0	-	$d_{bd}$	42.8	55.5	39.6	42.5	43.9	46.7	37.7	37.1
			$d_{bd}^{cone}$	41.2	49.7	36.4	37.7	40.9	43.7	36.0	36.7
	> 0	1	$d_{bd}$	58.2	69.2	51.7	54.4	40.9	45.9	33.6	35.8
			$d_{bd}^{cone}$	57.9	65.3	52.3	54.7	36.8	41.7	31.6	34.6
		2	$d_{bd}$	62.5	<u>71.8</u>	<b>58.4</b>	<b>59.1</b>	41.7	45.8	34.8	37.7
			$d_{bd}^{cone}$	<u>62.7</u>	67.7	<u>54.3</u>	<u>55.1</u>	40.7	45.7	34.6	36.7

## F. Experiments Setting

**Hyperparameters** In our experiments, we explored various hyperparameter configurations, focusing primarily on performance in low-dimensional spaces. Following the setup in (Yu et al., 2024), we evaluated our models in dimensions 5 and 10. The weighting coefficient  $\lambda$  in Eq. 7 was selected from  $\{0, 0.5, 1\}$ , while the learning rate was tuned over  $\{0.01, 0.005, 0.001, 0.0005\}$ . For the small dataset of mammals, which contains approximately 1000 nodes, we choose batch sizes from  $\{32, 64, 128\}$ . For the remaining datasets, we opt for batch sizes from  $\{1024, 2048, 8192\}$ . For the depth distance, we tested  $p \in \{1, 2\}$  as specified in Definition 2. The boundary distance margins in Eq. 4 were set to  $\gamma_1 = 0.001$  and  $\gamma_2 = 0$  for directed acyclic graph (DAG) embedding tasks. In ontology embedding experiments, both margins were set to zero.

For DAG experiments, as in (Yu et al., 2024), we trained for 400 epochs on the mammal and noun datasets and 500 epochs on the MCG and Hearst datasets. For ontology embedding experiments, we trained for 5000 epochs, following the protocol in previous work (Jackermeier et al., 2024).

**Ablation Studies** The results of the ablation studies are summarized in Table 5. Note that, when  $\lambda = 0$ , the depth distance component is absent from the energy function, and therefore, the choice of  $p$ , as a hyperparameter of depth distance, is not applicable.

From the results, it is evident that our boundary distance generally outperforms the specific boundary distances for boxes and balls (i.e.,  $d_{vol}$  and  $d_{bd}^{cone}$ ) in most cases. Furthermore, when using boxes as the embedding object, setting  $p = 1$  yields better results than  $p = 2$ . However, for balls,  $p = 2$  achieves superior performance.

For the mammal and noun datasets, using balls as the embedding object and incorporating the depth distance (i.e.,  $\lambda > 0$ ) in the energy function results in better performance. Conversely, for the MCG and Hearst datasets, the best performance is typically achieved when using boxes as the embedding region and setting  $\lambda = 0$ , effectively excluding the hyperbolic components. This observation aligns with our analysis in the main text.

It is worth noting, as shown in the seventh row of Table 5, that while the results using the depth distance are not always the best, they are very close to the best performance. This suggests that our depth distance configuration has the potential to achieve even better results with further refinement.

### F.1. Other Results

**Including non-basic edges in training** We evaluated the impact of including different percentages of transitive closure edges in the training set using the mammal dataset. The results, presented in Table 6, demonstrate that our method achieved



Table 6. F1 score (%) on mammal sub-graph with best numbers **bolded**. Results with \* are coming from Yu et al. (2024).

Non-basic-edge Percentage	Dimension = 2					Dimension = 5				
	0%	10%	25%	50%	90%	0%	10%	25%	50%	90%
GBC-box*	23.4	25.0	23.7	43.1	48.2	35.8	60.1	66.8	83.8	<b>97.6</b>
VBC-box*	20.1	26.1	31.0	33.3	34.7	30.9	43.1	58.6	74.9	69.3
$\tau$ Box	29.0	33.0	41.2	49.6	53.5	33.5	37.5	45.0	58.9	64.0
Entailment Cone*	54.4	61.0	71.0	66.5	73.1	56.3	<u>81.0</u>	<u>84.1</u>	83.6	82.9
ShadowCone (Umbral-half-space)*	57.7	<u>73.7</u>	<b>77.4</b>	<u>80.3</u>	79.0	69.4	<b>81.1</b>	83.7	<b>88.5</b>	<u>91.8</u>
Ours (box)	<b>64.9</b>	<b>74.4</b>	75.8	78.3	82.8	71.6	77.8	83.2	87.6	87.0
Ours (ball)	<u>62.7</u>	68.3	<u>77.2</u>	<b>84.1</b>	<b>88.6</b>	<b>71.8</b>	74.5	<b>84.4</b>	<u>88.4</u>	90.2

overall superior performance compared to existing approaches. This was particularly evident when the dimension was 2, where our method outperformed all other approaches across all conditions except with 25% non-basic edges—and even then, our F1-score was only 0.2 lower than the best performer. Our method exhibited more stable performance characteristics, with F1-scores increasing gradually as we added non-basic edges to the training set. In contrast, the current state-of-the-art method, ShadowCone, showed sharp initial improvements followed by diminishing returns. Specifically, when increasing non-basic edges from 0% to 10%, ShadowCone’s F1-scores jumped dramatically (increasing by 16.0 and 11.7 points for dimensions 2 and 5, respectively). However, further increases from 10% to 25% yielded much smaller improvements (3.7 and 2.6 points for dimensions 2 and 5, respectively).

**Using learnable function  $h$  in Equations 2 and 3** We investigated alternative formulations of the function  $h$  beyond using a constant value. Specifically, we evaluated two approaches:

1.  $h(reg) = 1/f_{MLP}([para(reg_1)])$
2.  $h(reg) = f_{MLP}([para(reg_1)])$

where  $f_{MLP}$  denotes a two-layer neural network defined as:

$$f_{MLP}(x) = \text{SoftPlus} \left( W^{(2)} \text{ReLU}(W^{(1)}x + b^{(1)}) + b^{(2)} \right)$$

The SoftPlus activation function ensures the positivity of  $h(reg)$ . In the implementation, we only use the center of balls and boxes as the input of  $h$ .

Our experimental results demonstrated that a constant value of  $h(reg) = 1$  generally achieved optimal performance across most scenarios. Neural network-based formulations of  $h(reg)$  showed advantages only in specific cases, such as with the heart dataset. For instance, when  $d = 5$ ,  $p = 2$ , and  $\lambda > 0$ , using  $h(reg) = 1/f_{MLP}$  improved the F1-score from 34.8 to 37.7 (see Table 5, intersection of the second-to-last row and second-to-last column). These findings suggest that while adaptive formulations of  $h(reg)$  can offer marginal improvements in specific scenarios, they require careful consideration in both design and training. For hierarchy-specific tasks, the simpler constant formulation of  $h(reg)$  typically provides sufficient and stable performance.

## F.2. Ontology embedding methods

**Implementation of ELBE and ELEM over DAG** As discussed in the main text, the ontology embedding methods ELBE and ELEM can be adapted to serve as baseline methods for embedding DAGs using boxes and balls, respectively. Specifically, for a pair of nodes  $(u, v)$ , the energy function used during training is defined as follows:

1. **ELBE:** Nodes  $u$  and  $v$  are embedded as boxes  $box_u$  and  $box_v$ , respectively. The energy function is given by:

$$E(u, v) = \|\max\{|\mathbf{c}_u - \mathbf{c}_v| + \mathbf{o}_v - \mathbf{o}_u, \mathbf{0}\}\|,$$

where  $\mathbf{c}_u$  and  $\mathbf{c}_v$  denote the center vectors of the boxes, and  $\mathbf{o}_u$  and  $\mathbf{o}_v$  denote the offsets of the boxes.

2. **ELEM:** Nodes  $u$  and  $v$  are embedded as balls  $ball_u$  and  $ball_v$ , respectively. The energy function is defined as:

$$E(u, v) = \max\{\|\mathbf{c}_u - \mathbf{c}_v\| + r_v - r_u, \mathbf{0}\},$$

where  $\mathbf{c}_u$  and  $\mathbf{c}_v$  represent the centers of the balls, and  $r_u$  and  $r_v$  represent their radii.

Note that the original ELEM method includes a regularization term that enforces the norms  $\|\mathbf{c}_u\|$  and  $\|\mathbf{c}_v\|$  to be close to 1. However, for the DAG case, we omit this regularization primarily applies to scenarios involving relation embeddings, such as axioms of the form  $A \sqsubseteq \exists r.B$  or  $\exists r.B \sqsubseteq A$ , as in the KGE methods TransE (Bordes et al., 2013).

**Integration of ELBE and ELEM with RegD and  $\tau$ Box** ELBE and ELEM are embedding approaches for normalized  $\mathcal{EL}$ -ontologies, which consist of four types of axioms  $C \sqsubseteq D$ :

$$A \sqsubseteq B, \quad A \sqcap B \sqsubseteq B', \quad A \sqsubseteq \exists r.B, \quad \exists r.B \sqsubseteq A.$$

ELBE embeds each atomic concept  $A$  as a box  $box(A) \subseteq \mathbb{R}^n$  and maps complex concepts like  $\exists r.B$  to a new box obtained by translating  $box(B)$  by a vector  $\mathbf{v}_r \in \mathbb{R}^n$ :

$$box(\exists r.B) = \{\mathbf{x} - \mathbf{v}_r \mid \mathbf{x} \in box(B)\}$$

ELEM employs a similar approach but uses balls instead of boxes. The key differences between ELBE and ELEM are as follows:

1. ELEM includes a regularization term, similar to TransE, to constrain the norm of the center of each ball to be close to 1.
2. ELBE handles conjunctions more effectively, as the intersection of two boxes is still a box. This allows it to define  $box(A \sqcap B)$  as  $box(A) \cap box(B)$ . In contrast, ELEM, which uses balls, cannot handle intersections directly and must use specialized mechanisms to approximate satisfaction of the axiom  $A \sqcap B \sqsubseteq B'$ .

To integrate RegD and  $\tau$ Box into ELBE or ELEM, it suffices to replace their energy function for axioms  $C \sqsubseteq D$  with the corresponding energy function from RegD or  $\tau$ Box. However, ELBE and ELEM handle negative samples differently, using a loss function of the form:

$$\mathcal{L} = \sum_{(C,D) \in P} E(D, C) + \sum_{(C',D') \in N} (\gamma - E(D', C')).$$

When integrating with RegD, this loss function should also be replaced with the one defined in Section 5.